

SANS and dynamic light scattering to investigate the viscosity of toluene under high pressure up to 1800bar

G Meier¹, J Kohlbrecher², R Vavrin²,

J Buitenhuis¹, M P Lettinga¹

and M Ratajczyk³

1: IFF, weiche Materie, FZ-Jülich, Postfach 1913, 52428 Jülich, Germany

2: Laboratory for Neutron Scattering, ETH Zurich & Paul Scherrer Institut, 5232 Villigen
PSI, Switzerland

3: Institute of Physics, A. Mickiewicz University, Umultowska 85, 61-614 Poznan, Poland

Abstract

We present a joint experimental study of small angle neutron scattering, SANS and dynamic light scattering, DLS under high pressures up to 1800bar on a colloidal suspension, which consists of a core-shell system made of sterically stabilized silica particles grafted with octadecyl chains in toluene. From the analysis of a SANS contrast variation under pressure we could estimate the amount of compression both in core and shell under the action of pressure. The DLS measurements under pressure yield a diffusion coefficient which enabled us together with the SANS result to evaluate the pressure dependent viscosity of the dilute suspension which is to a good approximation the solvent viscosity on the basis of the Stokes-Einstein relation. The excellent comparison of the so calculated pressure dependent viscosities of toluene with literature values demonstrates the value of our method to measure viscosities under pressure.

1. Introduction

The knowledge of accurate viscosity data of liquids over a wide range of temperatures and pressures is highly desired in order to design and possibly optimize materials in the lubricant industry. The viscosity of a lubricant has a tremendous effect on wear because of its relation to film thicknesses in bearings, where large hydrostatic pressures act [1]. The dynamic aspects of this are usually named elasto-hydrodynamic lubrication and are subject of novel research [2]. To measure viscosities under pressure is not an easy task, since it needs to have a pressure vessel, in which typically a falling ball viscometer is mounted. There are several experimental sophistications to this method and interpretation of the data is not straightforward due to the size effects of ball and container [3-6]. In this paper we adopt dynamic light scattering (DLS), to measure the pressure dependence of the diffusion of a colloidal particle of only about 40 nm in radius and by that the possibility to use it as a tracer particle to measure the viscosity of the solution by applying the Stokes-Einstein relation. To do so, of course also the size of the particle as a function of pressure must be known. Since the test particle is small and its concentration is low, we used small angle light scattering (SANS) to characterize this effect because the q -range is appropriate. Moreover, we have employed a contrast variation under pressure because only by that subtle procedure we are sensitive enough to detect small changes in size accurately. As a demonstration of the technique we compare our results for the pressure dependence of the viscosity with literature values and will discuss the limits of our experiment. The system we use consists of sterically stabilized silica particles which are grafted by octadecyl chains. This system forms stable dispersions in toluene and has been fully characterized by Kohlbrecher et al.[7]. The excellent agreement between literature values of the pressure dependent viscosity of toluene and those obtained by the combination of DLS and SANS at high pressures shows that the combination of these two methods

constitute a powerful micro-rheological tool at high pressures. Moreover, we will show that the silica particle is barely compressible and therefore a useful tracer particle for this purpose.

2. Dynamic light scattering DLS at high pressures

The time photon correlation functions of scattered light were measured as a function of temperature and pressure using a homemade high pressure setup which basically consists of the optical high pressure cell which is described elsewhere [8]. This high pressure cell works in a temperature range between -20°C and 120°C at pressures up to 2 kbars. The pressure transmitting medium is gaseous nitrogen. This is feasible, since the diffusion coefficient of nitrogen in a liquid (and also our sample) at ambient conditions is about $10^{-5} \text{ cm}^2/\text{s}$ and it thus takes a long time for the gas to diffuse into the optical cell filled up usually 2 cm above the laser beam level. Consequently, the measurements are safe with regard to softening of the sample with gas. The optical windows are made of a SF 57 NSK glass (Schott) which neither scrambles nor depolarizes the incident laser beam under conditions of high pressure. The scattering angle was $\theta = 90^{\circ}$ and the argon-ion laser (Spectra Physics) wavelength was 514.5 nm. A mono-mode optical fibre was used to feed the scattered light into an avalanche photodiode (Perkin-Elmer) working in photon counting mode. The intensity time-correlation function $G^{(2)}(q,t)$ was calculated in real time by means of an ALV 5000E digital correlator (ALV). For the homodyne case the intensity autocorrelation function $G^{(2)}(q,t) = \langle I(q,t)I(q,0) \rangle$ is related to the electric field, $E(q,t)$, normalized autocorrelation function $g^{(1)}(q,t)$ via the Siegert relation [9] .

$$G^{(2)}(q,t) = \langle I \rangle^2 \left(1 + f |g^{(1)}(q,t)|^2 \right) \quad (1)$$

where f is an experimental factor and $\langle I \rangle$ is the mean intensity and q being the magnitude of the scattering vector $|\mathbf{q}| = q = \frac{4\pi n}{\lambda} \sin \frac{\theta}{2}$. Here λ is the wavelength, n the refractive index and θ the scattering angle. Usually the normalized intensity autocorrelation function is calculated via $\hat{G}^{(2)}(q,t) = G^{(2)}(q,t) / \langle I \rangle^2$. Examples for this quantity for two pressures are shown in figure 1. One clearly sees that the correlation function is only shifted along the time axes under the action of pressure without any change in shape. $\hat{G}^{(2)}(q,t)$ has the full contrast which means that all concentration fluctuations relax in the time window of the experiment. With regard to the experimental factor f appearing in equation (1), usually this factor f is one to a good approximation using modern mono mode fibre techniques. The field autocorrelation function $g^{(1)}(q,t)$ is related in the simplest case of low concentration

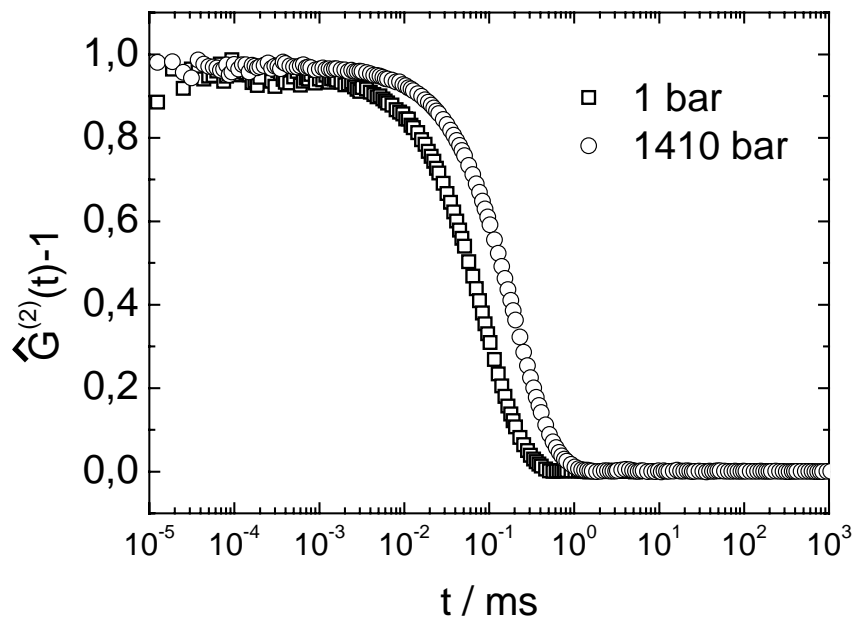


Figure 1. Normalized intensity autocorrelation function from a 0.05% solution of silica particles in toluene at $T=19.6^\circ\text{C}$ at $P=1\text{bar}$ and $P=1410\text{bar}$.

to a diffusion coefficient D of the system with equilibrium concentration fluctuations via $g^{(1)}(q, t) = \exp(-Dq^2t)$. This is usually written as $g^{(1)}(q, t) = \exp\left(-\frac{t}{\tau}\right)$, where τ is the decay time. To model the field autocorrelation function $g^{(1)}(q, t)$ in our case, where the system is not perfectly mono-disperse in size and thus we have a distribution in the diffusion coefficients. Therefore we used the CONTIN algorithm which is well established in analysing dynamic light scattering data. CONTIN gives access to the distribution of decay times $L(\tau)$ via [10]

$$g^{(1)}(q, t) = \int_0^{\infty} \exp\left(-\frac{t}{\tau}\right) L(\tau) d\tau \quad (2)$$

From the knowledge of $L(\tau)$ the first moment of the distribution is calculated according to

$$\bar{\tau} = \frac{\int_0^{\infty} \tau L(\tau) d\tau}{\int_0^{\infty} L(\tau) d\tau} \quad (3)$$

The distribution of decay times is related to a distribution of diffusion coefficients and thus to the size distribution of the particles since D is related to size via the Stokes-Einstein relation

$$D = \frac{kT}{6\pi\eta r} \quad (4)$$

with η being the solvent viscosity and r the hydrodynamic particle radius, kT has the usual meaning. The data for $P=1\text{bar}$ yielded a particle size of $r=39.5\text{nm}$ from the unweighted CONTIN analysis in agreement with previously published value by Kohlbrecher et al. [7]. We had found that all SANS data were in good agreement with a size distribution of the particles with a relative width of $\sigma=0.13$, cf. equation (10). Equation (4) is written without any pressure dependence. Taking that into account, it then reads:

$$\frac{1}{2q^2(P)\tau(P)} = D(P) = \frac{kT}{6\pi\eta(P)r(P)} \quad (5)$$

Note that q depends on pressure for a fixed scattering angle because the refractive index n depends on P . This correction has to be taken into account properly. DLS measurements give access to $\tau(P)$ and thus to $D(P)$. In figure 2 we plot the first moment of the decay time distribution obtained from the CONTIN analysis according to equation (3), $\bar{\tau}(P)$ as a function of pressure. We should note here that it does not matter whether we plot $\tau(P)$ or $\bar{\tau}(P)$, because the shape of $\hat{G}^{(2)}(q,t)$ does not change with pressure, as is evidenced from figure 1. The magnitude of the observed effect is about a factor of 2 in the decay time per kbar. In the following sections we will address the pressure dependence of $r(P)$ and $q(P)$ in order to finally derive the desired pressure dependence of the viscosity $\eta(P)$.

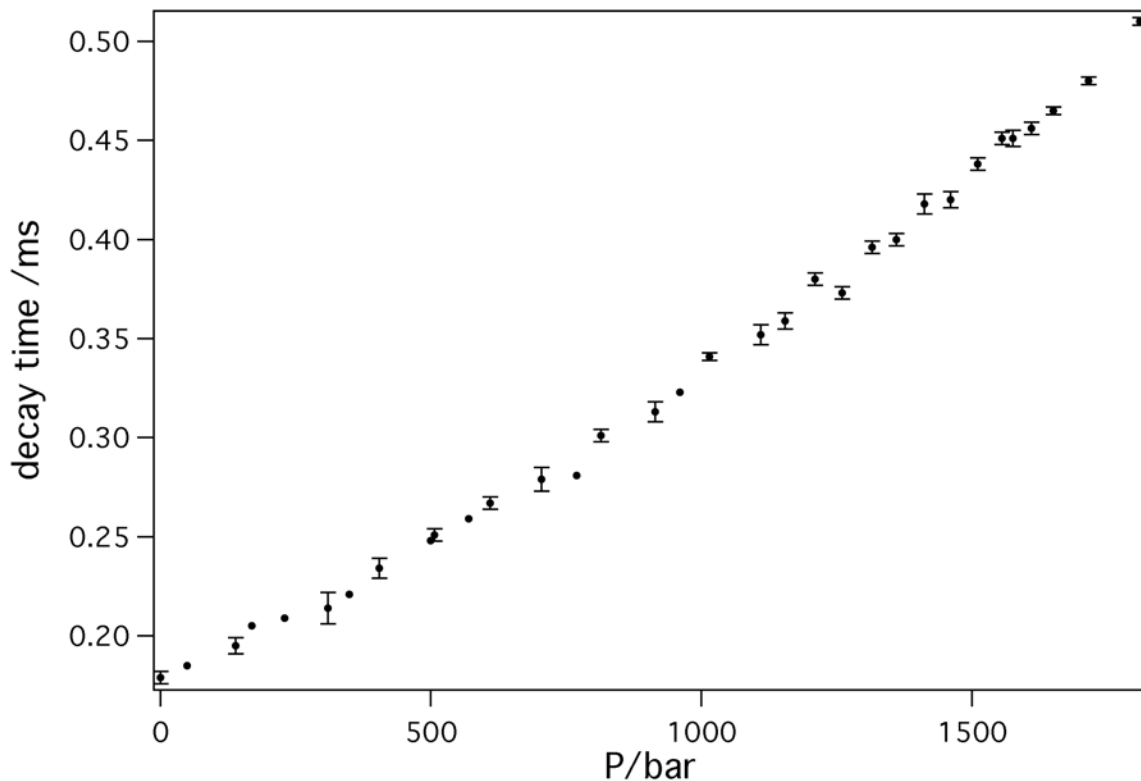


Figure 2. Pressure dependence of the first moment of the distribution of decay times from a CONTIN analysis as obtained from DLS measurement from a 0.05% solution of octadecyl grafted silica spheres in toluene at $T=19.6^\circ\text{C}$. Most of the points were measured about 5 times to assure proper statistics. The statistical error per point is about 3%.

3. Pressure dependence of particle radius analysed by SANS

We have performed the SANS experiments at the SANS I instrument at the SINQ spallation source at the Paul Scherrer Institute (PSI) in Villigen, Switzerland [12]. We used thermal neutrons of wavelength $\lambda = 0.8$ nm with a wavelength spread $\Delta\lambda/\lambda$ of about 0.1. The data analysis was performed using the BerSANS software package [13] which accounts for all necessary corrections due to background, transmission, sample thickness, count rate/dead time ratio, masking and radial averaging of the raw data. A standard water sample was used for calibration to absolute scattering intensities and also to account for a non-uniform detector efficiency [14].

We have performed SANS scattering experiments from a 5% solution of the colloid in toluene for a series of pressures with varying scattering length density of the solvent around the match point, which masks the scattering length density of the core for the contrast variation. These high pressure measurements have been performed with a custom made high pressure cell suitable for SANS, which is available at the PSI [15]. For our core-shell particles the form-factor is known analytically. For this volume fraction we observe a weak structure factor, which can be well described in terms of a sticky hard sphere structure factor for polydisperse systems as shown by Kohlbrecher et al. [7].

For dilute dispersions, the expression for the determination of the measured intensity $I(q)$ from a SANS experiment is given by the coherent macroscopic cross section $d\Sigma_{coh}/d\Omega(q)$ plus an incoherent macroscopic cross section $d\Sigma_{inc}/d\Omega$, which does not depend on q . Thus we have

$$I(q) = \frac{d\Sigma_{total}}{d\Omega}(q) = \frac{d\Sigma_{coh}}{d\Omega}(q) + \frac{d\Sigma_{inc}}{d\Omega} = N_p \langle F_{cs}^2(q) \rangle + I_{inc} \quad (6)$$

where N_p denotes the number density of particles, I_{inc} the q -independent background and the $\langle \dots \rangle$ the average over the form amplitudes $F(q)$.

We deal with core-shell particles, which consist of an inner core with radius r_c and uniform scattering length density ζ_c . The core is surrounded by a shell of uniform thickness Δr and scattering length density ζ_s , so

$$\zeta(r') = \begin{cases} \zeta_c & \text{for } r' \leq r_c \\ \zeta_s & \text{for } r_c < r' < r_c + \Delta r \end{cases} \quad (7)$$

where r' is the distance from the centre of the particle. Then we yield the following expression for the particle form amplitude $F_{cs}(q)$ of a core-shell particle:

$$F_{cs}(q, r_c, \Delta r) = (\zeta_c - \zeta_s) F(q, r_c) + (\zeta_s - \zeta_m) F(q, r_c + \Delta r) \quad (8)$$

with $r = r_c + \Delta r$ is the total radius of core plus shell (note that this r differs from the r' in equation (7) and the $F(q, r)$ is given by

$$F(q, r) = \frac{4}{3} \pi r^3 \frac{3 [\sin(qr) - qr \cos(qr)]}{(qr)^3} \quad (9)$$

In a contrast variation experiment, where the scattering length density of the solvent ζ_m is varied, different situations can be obtained: if we chose $\zeta_s \approx \zeta_m$ (which means, we match out the shell), the second term in equation (8) is zero and we observe the form amplitude of the core. On the other hand, if $\zeta_c \approx \zeta_m$ (we match out the core), then only the scattering contribution described by the form amplitude of the shell remains. This regime is therefore most sensitive for obtaining information on the scattering length distribution within the shell structure. Our

colloidal particle system under study is dissolved in toluene, which is a mixture of the protonated and deuterated solvent. From the respective numerical values for these scattering length densities (toluene-d8: $\zeta=5.66 \times 10^{10} \text{cm}^{-2}$, toluene-h8: $\zeta=0.94 \times 10^{10} \text{cm}^{-2}$) one can see that there is no combination of solvents which will mask out the shell with a negative scattering length density of $\zeta=-0.23 \times 10^{10} \text{cm}^{-2}$. But since the core ($\zeta=2.4 \times 10^{10} \text{cm}^{-2}$) can be matched out, the shell alone can be seen. Our particles have a size distribution and therefore we assumed a Schulz-Zimm distribution for the overall radius $r=r_c+\Delta r$, whereas the corona thickness is supposed to be fixed. This distribution function $L(r)$, which we have to insert in equation (6) for $r_c+\Delta r$ reads:

$$L(r) = \frac{N}{R_a} \left(\frac{r}{R_a} \right)^{k-1} k^k \exp\left(-k \frac{r}{R_a}\right) \frac{1}{\Gamma(k)} \quad \text{with } k = \frac{1}{\sigma^2} \quad (10)$$

where the normalisation is given by $\int_0^{\infty} L(r) dr = N$. The variance σ^2 is a measure of the width of the distribution, R_a is a scaling parameter which defines the maximum of the size distribution for small values of σ and Γ denotes the gamma function.

In figures 3a-f we show the results of the contrast variation measurements under high pressures. We have measured at 1bar, 400bar, 700bar, 1kbar, 1.3kbar and 1.6kbar at scattering length densities of the solvent ranging from $\zeta=1.9, 2.1, 2.2$ to $2.4 \times 10^{10} \text{cm}^{-2}$. In the global fit procedure we have set the following parameters free: parameters entering equation (10), N , R_a and σ , the compressibility of the particle and the product of shell thickness times amount of solvent in it. The parameters obtained were the same as those published previously [7].

However, we have multiplied the scattering length density of the solvent ζ_m with the change of density as a function of pressure according to $\zeta_m(P) = \zeta_m(1\text{bar}) \frac{\rho(P)}{\rho(1\text{bar})}$ in order to get the

true scattering length density difference at a given pressure between solvent and particle. To do so we have interpolated the data by Harris [16] for the pressure dependent density of toluene at the temperature of the SANS measurement of $T=16^{\circ}\text{C}$. These values for the density can be fitted using a 2nd order polynomial fit according to $\rho(P) = 0.873 + 5.65 \cdot 10^{-5} P - 5.272 \cdot 10^{-9} P^2$ with P/bar and ρ in g/cm^3 . If we assume a linear relation between the volume of the core and its variation with pressure according to $V(P) = V_0(1 - \kappa_T P)$, which recovers upon differentiation with regard to P the definition of the isothermal compressibility κ_T , then we can determine through the global fit routine the scattering length density of the core ζ_c as a function of pressure by assuming $\zeta_c(P) = \zeta_{c,1\text{bar}} / (1 - \kappa_T P)$. The fit gave values for the isothermal compressibility κ_T in the order of $5 \times 10^{-6} \text{ bar}^{-1}$. Thus, from the change of scattering length density with pressure we can conclude that the equivalent change in volume corresponds to a hypothetical change in radius of about 0.07nm. From the corona in principle also a compression effect is conceivable, however, we had found the Δr constant in our global fit and thus have to conclude that the corona configuration is not changed. As this geometrical correction is about two orders in magnitude smaller than the error in determining the first moment from CONTIN according to equation (3), we can safely consider them as being inconsequential and have therefore undertaken no geometrical correction.

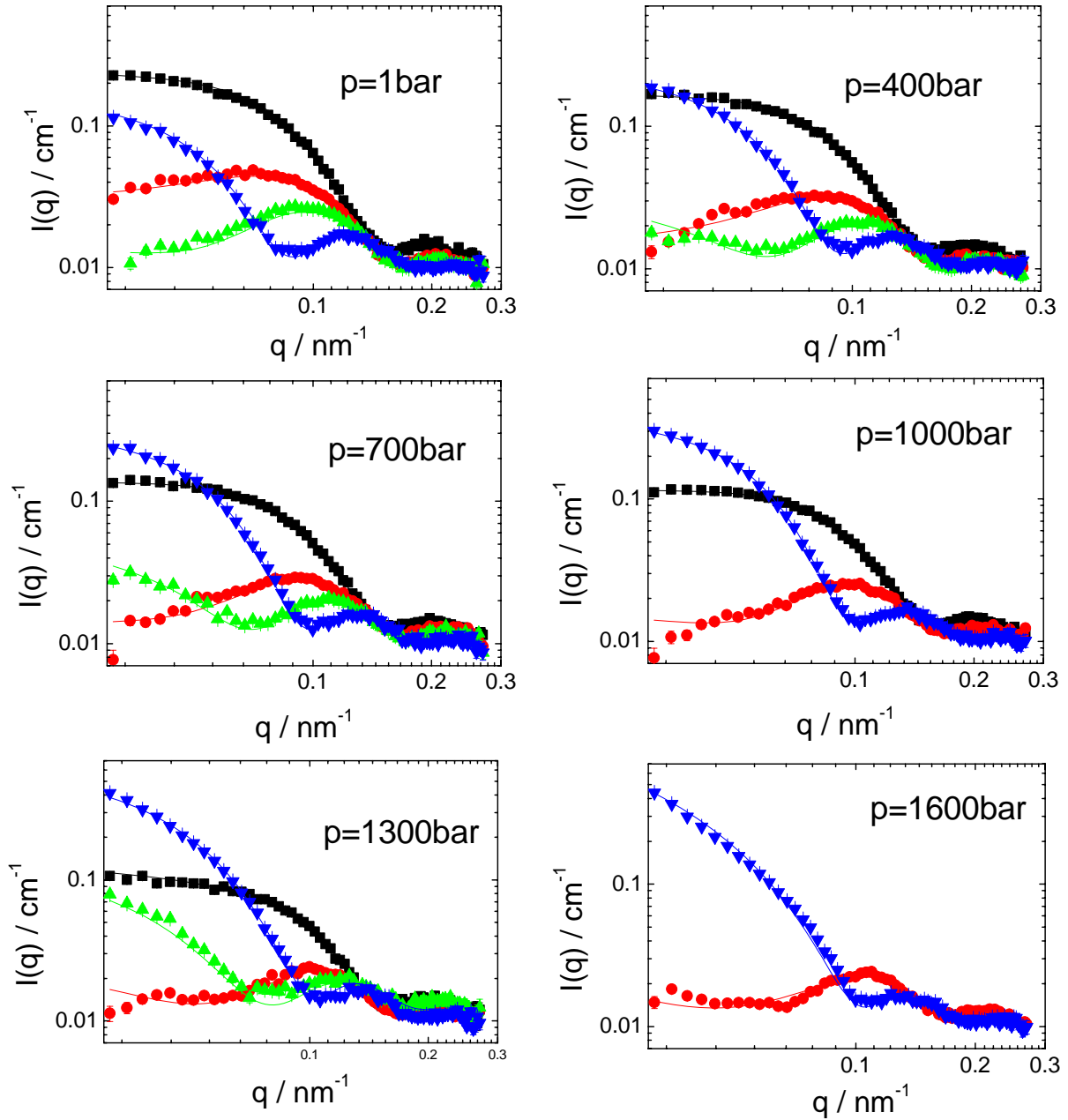


Figure 3a-f. from left to right and top to bottom with decreasing P . SANS contrast variation of 5% solution of silica particles in a mixture of h/d toluene with scattering length density $\zeta=1.9 \times 10^{10} \text{cm}^{-2}$ (squares), $\zeta=2.1 \times 10^{10} \text{cm}^{-2}$ (circles), $\zeta=2.2 \times 10^{10} \text{cm}^{-2}$ (triangles up), $\zeta=2.4 \times 10^{10} \text{cm}^{-2}$ (triangles down). Full lines are results of global fits according to equations (8,9) taking the size distribution according to equation (10) into account.

4. Pressure dependent refraction index

The light scattering data shown in figure 1 have been obtained at a fixed scattering angle of $\theta=90^\circ$. However, measuring $D(P)$ needs to take the pressure dependence of the magnitude of the scattering vector q into account, because the refractive index n depends on pressure, cf. equation (5). Usually the pressure dependence of n is discussed in terms of the Clausius-Mosotti equation and modifications of it, as discussed by Vedam and Limsuwan [17]. In any case, proportionality between n^2 and density is found in first order and is supported by literature data on both density [16] and n [18] as a function of pressure. To be more specific, we calculate the ratio between $n^2(P)$ and $n^2(1bar)$ following reference [17] using the Lorentz-

Lorenz equation $\frac{n^2 - 1}{n^2 + 2} = \frac{4\pi\alpha}{3M_w N_A} \rho$ where α is the electronic polarizability and ρ the density:

$$\frac{n^2(P)}{n^2(1bar)} = \frac{1 + 2C\rho(P)}{1 + 2C\rho(1bar)} \frac{1 - C\rho(1bar)}{1 - C\rho(P)} \quad (11)$$

where the constant C is given by the relation $C = \frac{1}{\rho(1bar)} \left(\frac{n^2(1bar) - 1}{n^2(1bar) + 2} \right)$.

For the pressure dependence of the density at $T=19.6^\circ\text{C}$ we have interpolated the data by Harris [16]. These values can be well approximated using a 2nd order polynomial fit according to $\rho(P) = 0.87 + 5.72 \cdot 10^{-5} P - 5.34 \cdot 10^{-9} P^2$ with P/bar and ρ in g/cm^3 .

5. Discussion

The pressure dependence of the viscosity can now be extracted from the DLS data, knowing the pressure dependence of the refractive index, which is accessible via the pressure dependence of the density. Starting from equation (4) with the help of equation (11), we can write the ratio between $\tau(1bar)$ and $\tau(P)$ as

$$\frac{\tau(P)}{\tau(1bar)} \frac{n^2(P)}{n^2(1bar)} = \frac{\eta(P)}{\eta(1bar)} \quad (12)$$

remembering $\tau^{-1} = Dq^2$. Using the viscosity value for toluene at 1bar, we can calculate the pressure dependence of the viscosity from eq.12. This result is shown in figure 4. The viscosity given by Harris [16] was interpolated for all temperatures to the measured pressures. At each given pressure, the viscosity for the temperature of 19.6 °C was then calculated by interpolating the values for all temperatures using a 2nd order polynomial fit. The relative viscosities in figure 4 can thus be approximately described by $\eta(P) = \eta(1\text{bar}) [1 + 7.13 \cdot 10^{-4} P + 2.23 \cdot 10^{-7} P^2]$.

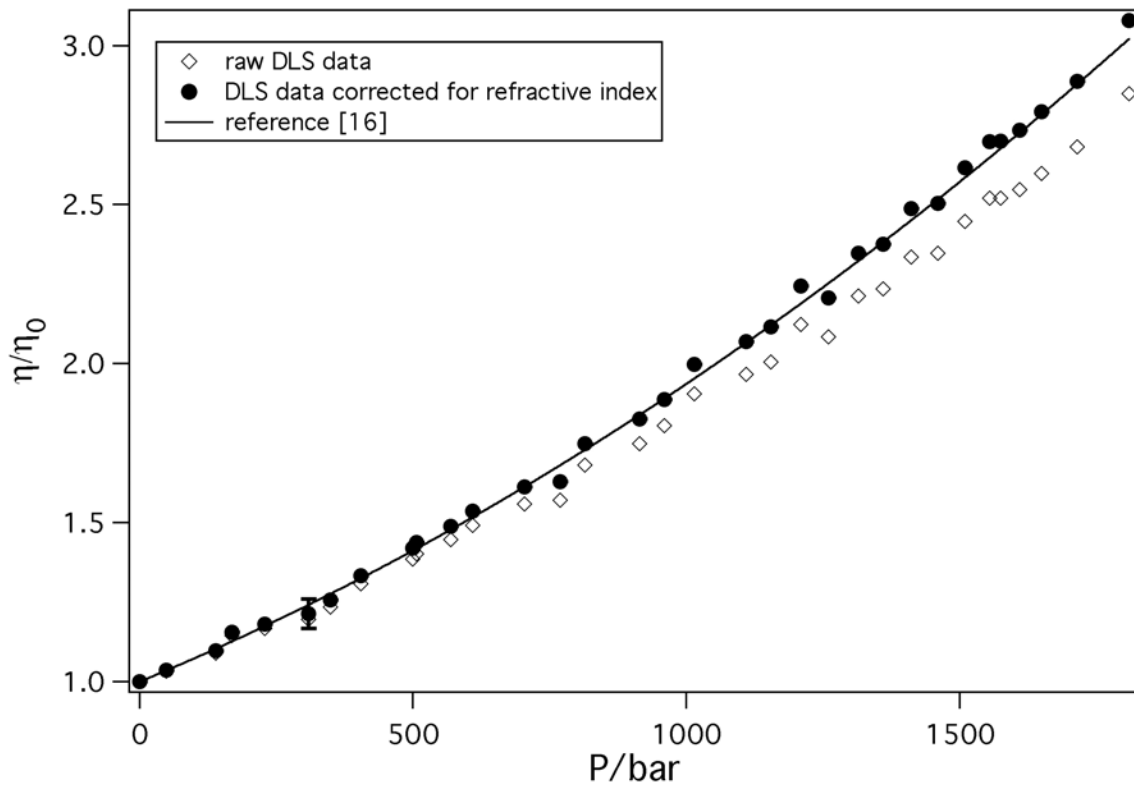


Figure 4. The relative change of viscosity of toluene with pressure at $T=19.6^\circ\text{C}$ as obtained from DLS, raw data see figure 1, by applying equation (12) compared to the literature values, line [16]

As one can see, the agreement is excellent. It shows that the proposed method is a kind of micro-rheological viscometer to evaluate the pressure dependent viscosity. The advantages of the procedure are its simple experimental setup and straightforward analysis as compared to a falling ball viscometer. Another advantage of our procedure is the small sample amount needed. A typical DLS measurement is possible to work with volumes smaller than 1ccm.

The compressibility of the tracer particle can be an issue, but we have shown here that silica colloids hardly shrink and since pure silica can be nicely dispersed in water it can be a useful tracer also for biological systems. Also some proteins like for example glucose isomerase were found to be remarkably stable under high pressure conditions [19] and can thus serve as a perfect test particle for the determination of the pressure dependence of the solvent viscosity, which is in that case basically a water/buffer solution. So we are rather confident that not only hydrophobic organic solvents can be measured but likewise aqueous systems which play an important role in deep ocean research and related fields.

There is however still some concern connected to the evaluation of the absolute value of the viscosity. As one can see from equation (4), there must be two quantities known in order to determine the viscosity: the diffusion and the geometry. Concerning DLS there is always a debate how the geometry of a diffusing particle is related to its diffusing volume. Strictly in equation (4) the so called hydrodynamic radius enters and thus a hydrodynamic volume, which is always larger than the geometrical volume for particles with no penetration by solvent molecules. Since the ratio between hydrodynamic to geometrical volumes depends on the nature of the underlying interactions, no clear prediction of the absolute value for the viscosity is possible [20].

Next we have to consider the limits of applicability of equation (4). Though the Stokes-Einstein relation is rather robust, one has to consider slip or stick boundary condition. Usually for large non-ionic particles stick boundary conditions are found, contrary to small ionic particles where slip boundary conditions are dominant. In that case the factor 6π in equation (3) is replaced by 4π . We do not find any hint for this slip behaviour in our data [21], moreover it seems intuitively clear that stick boundary are better realized the higher the pressure is.

5. Conclusion

We could show that performing DLS on a dilute solution of colloidal particles under pressure up to 1.8kbar is appropriate to measure the relative change of the solution viscosity by applying the Stokes-Einstein relation. The proposed method is in a sense a kind of micro-viscometer since our test particles are small. In order to use the method, one has to know first of all how the volume of the particle depends on pressure. In our case we have proven by a SANS contrast variation experiment that the particle compressibility is negligible. Next, because we propose an optical method, the index of refraction as a function of pressure is needed. We have used a Lorentz-Lorenz equation to account for $n(P)$ on the basis of pressure dependent density values from literature which is more easy accessible. Under the given assumptions one gets an easy access to relative viscosity changes under pressure within 3%.

Acknowledgements

The SANS data are based on experiments performed at the Swiss spallation neutron source SINQ, Paul Scherrer Institute, Villigen, Switzerland.

References

- [1] Lugo.L, Canet X, Comunas M J P, Pensado A S and Fernandez J 2007 *Ind. Eng. Chem. Res.* **46** 1826
- [2] Bair S, Jarzynski J and Winer W O 2001 *Tribology International* **34** 461
- [3] McLachlan R J 1976 *J. Phys. E: Sci. Instrum.* **9** 39
- [4] Dandridge A and Jackson D A 1981 *J. Phys. D: Appl. Phys.* **14** 829
- [5] Wong P L, Lingard S and Cameron A 1992 *STLE Trib. Trans.* **35** 500
- [6] King H E, Herbolzheimer E and Cook R L 1992 *J. Appl. Phys.* **71** 2078

- [7] Kohlbrecher J, Buitenhuis J, Meier G and Lettinga M P 2006 *J. Chem. Phys.* **125** 044715
- [8] Fytas G, Meier G and Dorfmueller Th 1986 *Macromolecules* **18** 993
- [9] Berne B J and Pecora R 1976 *Dynamic Light Scattering* Chapter4 (New York: Wiley)
- [10] Brown W 1993 *Dynamic Light Scattering* Chapter4 (Oxford: Clarendon Press)
- [11] Thomas J C 1986 *J. Colloid Interface Sci.* **117** 187
- [12] Kohlbrecher J and Wagner W 2000 *J. Appl. Cryst.* **33** 804
- [13] Keiderling U 2002 *Appl. Phys. A* **74** S1455
- [14] Stunz P, Saroun J, Keiderling U, Wiedenmann A and Przenioslo R 2000 *J. Appl. Cryst.* **33** 829
- [15] Kohlbrecher J, Bollhalder A, Vavrin R and Meier G 2007 *J. Appl. Phys.* Submitted
- [16] Harris K R 2000 *J. Chem. Eng. Data* **45** 893
- [17] Vedam K and Limsuwan P 1978 *J. Chem. Phys.* **69** 4772
- [18] Vedam K and Limsuwan P 1978 *J. Chem. Phys.* **69** 4762
- [19] Banachowicz E, Kozak M, Patkowski A, Meier G and Kohlbrecher J 2007 *J. Appl. Cryst.* **00** 0000
- [20] Brown W 1996 *Light Scattering: Principles and Development* Chapter13 (Oxford: Clarendon Press)
- [21] Alder B J, Gass D M and Wainwright T E 1970 *J. Chem. Phys.* **53** 3813